

# A computational docking study for prediction of binding mode of diospyrin and derivatives: Inhibitors of human and leishmanial DNA topoisomerase-I

Sandeep Chhabra, Pooja Sharma and Nanda Ghoshal\*

Structural Biology and Bioinformatics Division, Indian Institute of Chemical Biology (IICB), 4 Pura S.C. Mukherjee Road, Jadavpur, Kolkata 700032, India

Received 7 February 2007; revised 8 May 2007; accepted 15 May 2007  
Available online 31 May 2007

**Abstract**—A computational approach was utilized to study the relative binding modes of diospyrin (bisanaphthoquinonoid) with the crystal structure of human DNA–TopoI and the recently reported *Leishmania donovani* DNA–TopoI. Additionally, the binding site interactions of amino derivatives of diospyrin with human TopoI were studied extensively. Based on the docking results, binding modes of diospyrin with the human and leishmanial TopoI catalytic core were predicted. The parallel use of two efficient and predictive docking programs, GOLD and Ligandfit, allowed mutual validation of the predicted binding poses. A reasonably good correlation coefficient between the calculated docking scores and the experimentally determined cytotoxicity helped in validating the docking method. Furthermore, a structure-based pharmacophore model was developed for *L. donovani* DNA–TopoI inhibition which helped in elucidating the topological and spatial requirements of the ligand–receptor interactions. This study provides an understanding of the structural basis of ligand binding to the topoisomerase receptor, which may be used for the structure-based design of potent and novel ligands for anticancer and antileishmanial therapy. To our knowledge, this is the first report of a binding mode exploration study for diospyrin and its derivatives as inhibitors of the leishmanial and human TopoI enzymes.  
© 2007 Elsevier Ltd. All rights reserved.

DNA Topoisomerases are ubiquitous enzymes common to all living organisms. Topoisomerases are classified as type I and II on the basis of different sequences and functions. Topoisomerase I (TopoI) is an essential enzyme participating in all those processes associated with separation of DNA strands. This enzyme plays a pivotal role in modulating the DNA topology during replication, transcription, recombination, and repair, and has been established as potential target for rational design of anticancer and antileishmanial agents.<sup>1,2</sup> This is supported by the fact that *Leishmania donovani* (Ld) and human TopoI have sufficient biochemical and structural differences to enable selective targeting of the parasite and human enzymes.<sup>1</sup> Diospyrin (Fig. 1) is a plant product (bisanaphthoquinonoid) and a potent inhibitor of type I DNA topoisomerase, that has significant inhibitory effect on the growth of *L. donovani* as well as on murine tumor in vivo and human cancer cell lines

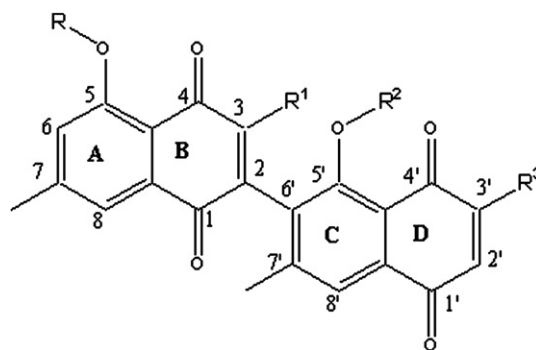


Figure 1. Common structure of diospyrin derivatives.

in vitro but with different potencies.<sup>3,4</sup> Thus there exists the potential of structure-based design for the development of selective, less toxic, and potent diospyrin analogues using in silico approaches.

Diospyrin and its amino derivatives were found to possess cytotoxicity against EAC tumor cells.<sup>5,6</sup> The SAR of these derivatives have recently been reported by our group suggesting that fragment-based sterimol param-

**Keywords:** Diospyrin; Human DNA–TopoI; *L. donovani* DNA–TopoI; Molecular docking; Structure-based pharmacophore.

\* Corresponding author. Tel.: +91 33 2473 3491x254; fax: +91 33 2473 0284/5197; e-mail: [nghoshal@iicb.res.in](mailto:nghoshal@iicb.res.in)

ters and spatial arrangements of bulky substituents, charged partial surface area, nucleophilicity and hydrophobicity parameter play significant roles in eliciting these activities for this class of compounds. This information was used for development of novel and potent diospyrin derivatives.<sup>6</sup> As diospyrin shows lesser but selective inhibitory activity<sup>1,7</sup> in *Ld*TopoI, structure based drug design (SBDD) or pharmacophore generation may lead to development of more potent compound of this series.

Prediction of the correct binding mode of each compound using docking programs is a key step if structure-based design is to be used for improving potency. Herein we report, for the first time, the relative binding mode of diospyrin with crystal structure of the human DNA–TopoI and the recently reported *Ld*DNA–TopoI using molecular docking. Our findings support the feasibility of specifically targeting *Leishmania* TopoI through rational drug design and contribute to the understanding of the modes of action of current antileishmanials.

The results obtained from this study reveal the dissimilarities in the binding mode of diospyrin with TopoI from human and *L. donovani* as well as are able to point out which interaction sites in the binding pocket might be responsible for the variance observed in the biological activities. The analysis of the best-docked conformations has been used to investigate the binding mode of compounds involved in this study, which in turn confirms the role of bulky substituents<sup>6</sup> and some amino acid residues<sup>19</sup> present in the active site of human DNA–TopoI. The proposed binding interaction of diospyrin with ‘predicted’ active site of *Ld*DNA–TopoI, in consideration of binding energies, hydrogen bonding, hydrophobic, and van der Waals interactions, points out the key features needed for structure-based design of more selective and less toxic diospyrin analogues.

The structures of 12 diospyrin derivatives were taken from our recently reported QSAR study.<sup>6</sup> The 3D-structures of the molecules were modeled by using Build/3d-sketcher module of Cerius2 v4.9.<sup>10</sup> The charges were calculated at the beginning and the charge method used was Gasteier.<sup>20</sup> Simple energy minimization does not guarantee global minimum (lowest energy conformation), for all the compounds, the conformation space was first scanned using energy optimization cycles followed by dynamic simulation using the annealing dynamics with user defined attributes-Reqttemp-500K, dynamic time step-0.001Ps, Steps-2000 using constant NVE (constant number of atoms, volume, and energy). This was followed by energy minimization procedure. The force field used was Universal 1.02<sup>11</sup> and the molecules were minimized to high convergence (cutoff value of energy difference 1.000E-3 kcal/mol) using 500 (or more if required) iterations on the smart minimizer. Eight to 10 runs were performed for each compound. The lowest energy structure thus obtained was taken as final model (Probable global minimum).

The Cerius2 (LigandFit v4.9)<sup>10</sup> and GOLD v3.01<sup>12</sup> Software were used to dock all the compounds into the

active site of the human DNA–TopoI (PDB: 1SC7)<sup>8</sup> and *Ld*DNA–TopoI (PDB: 2B9S)<sup>9</sup> structures. GOLD is a well-known automated ligand-docking program that uses a genetic algorithm (GA) to explore the full range of ligand conformational flexibility with partial flexibility of the protein side chains.<sup>13,14</sup> The binding site was defined to include all residues within 10 Å of the ligand in original complex of human DNA–TopoI. In this structure<sup>2</sup> TopoI is bound to the oligonucleotide sequence 5'-AAAAAGACTTsX-GAAAAATTTTT-3', where ‘s’ is 5'-bridging phosphorothioate of the cleaved strand and ‘X’ represents any of the four bases A, G, C or T. Protein preparation for the docking experiment included extraction of the ligands and the water molecules from the active site and addition of hydrogens using InsightII (Accelrys, San Diego, CA). The protonation state of charged groups was set assuming pH 7. The default calculation mode, which provides the most accurate docking results, was selected for all calculations. In the standard calculation mode by default, the GA run comprised of 100,000 generations on an initial population of 100 members divided into five sub-populations, and the annealing parameters of fitness function were set at 4.0 for van der Waals and 2.5 for hydrogen bonding. Default values were selected for other parameters as well. The number of generated poses was set to 100 and top ranked solutions were kept, with the early termination option turned off. Each compound was reported from a mol2 file. The Scoring function, GOLD Fitness Score was selected for each compound, as deemed appropriate.

LigandFit module in Cerius2 v4.9 was also used for the docking study and binding site search. LigandFit gives the best poses at the binding site by a stochastic conformational search and evaluation of the energy of the ligand–protein complex. It uses a grid method when evaluating interactions between the protein and the ligand. In our case the binding site search was performed in the shape-based mode (flood filling method) for both the enzymes. The second largest site searched by shape-based mode covered the X-ray ligand and was verified by the location of redocked X-ray ligand in the crystal structure of human DNA–TopoI. In case of *Leishmania*, the *Ld*TopoI<sub>LS</sub> (large subunit)–vanadate–DNA complex<sup>9</sup> was used. DNA and vanadate ion were removed from protein. For the *L. donovani* DNA–TopoI, we again used the protein shape-based method to define the binding site, as crystal structure of this enzyme did not have ligand coordinates. For initial exploration of binding site, various sites were searched and analyzed by docking of diospyrin to the *Ld*DNA–TopoI. Enlargement of the best ‘predicted’ site model (consisting of 4527 grid points) was done to cover the proposed ligand-binding region. The energy of the grid was set using CFF (v1.02) energy function with a resolution of 0.5 Å and opening size of the site 5 Å.<sup>15</sup> The ligand-accessible grid was defined such that the minimum distance between a grid point and the protein is 2.0 Å for hydrogen and 2.5 Å for heavy atoms. The grid extends from the defined active site to a distance of 3 Å in all directions. This grid was used to calculate the non-bonded interactions between all the atoms of ligands

and protein residues and non-bonded cutoffs were set to 10 Å. Although the solvation energies could not be explicitly considered during the minimization, the energy calculations were performed with a distance-dependent dielectric constant (5.0) to mimic the solvation effect of the inhibitors in the protein environment.<sup>16</sup> Diverse conformations were computed using the Monte Carlo algorithms. In order to obtain the best results the parameter of maximum saved conformers was finally set to ( $N_{\text{save}}$ ) = 60 with number of trials 99,999 (as these parameters were found sufficient to reproduce X-ray bound conformation in our previous docking study).<sup>17</sup> The SD file was used as an input file of the ligands. Additionally, a complex of *Ld*TopoI was employed to construct structure-based pharmacophore hypothesis, using Ligand Scout v1.03.<sup>18</sup> In this method structure of the receptor–ligand complex is used in order to extract relevant chemical features, intuitively derived from the complex. The 3-D pharmacophore concept is based on specifically those kinds of interactions that have been observed in drug–receptor interaction, viz. hydrogen bonding, charge transfer, electrostatic, and hydrophobic interactions. This spatial arrangement of chemical features represents the essential interactions of small ligands with a macromolecular receptor.

In the present study, the ligand-binding mode in human DNA–TopoI (with 12 compounds, Table 1) and *Ld*DNA–TopoI (with diospyrin) was established for the first time by studying direct ligand–receptor interactions in silico. Structures of the receptor–ligand complex predicted by LigandFit were ranked with built-in scoring functions in Cerius2.<sup>10</sup> As each scoring function may rank binding poses differently, a consensus scoring approach was used with six different scoring functions: (i) Dock score, (ii) Ligscore, (iii) PLP1, (iv) PLP2, (v) Potential mean force (PMF), and (vi) LUDI. Each predicted binding model was selected for further consideration in the next step if it was ranked in the top 10% by at least three of the six scoring functions. Models selected by LigandFit in this way were compared to those predicted by GOLD. If the root-mean-square-deviation (RMSD) between the corresponding heavy atoms for the ligand in predicted binding models was less than 2 Å, these binding models were considered to be in good agreement and retained for further evaluation. The final choice of the models was based on few considerations

such as interaction with key residues, correlation with biological activity, and above-mentioned RMSD between best pose from GOLD and LigandFit. GOLD was able to locate the same binding models found by LigandFit. This increased our confidence in the reliability of the predicted poses. We used only GOLD models for further discussion as those were in good agreement with LigandFit.

**Molecular-interaction with human topoisomerase-I.** Compounds 1–12 were first docked into the binding pocket of human TopoI. Earlier experiments showed that human TopoI is comprised of four major domains:<sup>19,20</sup> (i) NH<sub>2</sub>-terminal domain situated between Met1 and Lys197, and seems dispensable for in vitro activity, (ii) ‘Core domain’ formed by highly conserved residues Glu198 to Ile651, (iii) short/unconserved linker (Asp 652 to Glu696), and (iv) C-terminal domain, situated between Gln697 and Phe723, is highly conserved and contains the active site Tyr723. These studies also suggest that catalytic residues include Asn722, Lys532, Asp533, Arg364, Asn352, Arg488, Arg590, and Tyr723.

The docking analysis of diospyrin and its amino derivatives with human TopoI revealed some common features of inhibitors observed in earlier studies. It has been proposed that its action certainly results from a direct interaction with the enzyme and subsequent interference with campylochrom-dependent TopoI-mediated DNA cleavage, implying that diospyrin derivatives mediate a conformational change of topoisomerase.<sup>21</sup> Thus, in our study we used only TopoI after removal of DNA molecule from PDB complex. The optimized positions of polar protein hydrogen atoms and hydrogen-bond geometries that are generated during GOLD docking were saved as SD file tags and described here. This software uses genetic algorithm-based flexible docking that implicitly handles local protein flexibility by allowing a small degree of interpenetration or van der Waals overlap of ligand and protein atoms.

The best-docked structures for these ligands possess a number of common features. The naphthoquinone moiety (ringA/B) was found within H-bonding distance of Arg488, Arg 590, and Thr718 (essential residues). The binding modes of highly active compound 12 and moderately active compound 10 are shown in Figures 2 and

**Table 1.** General structures and experimental cytotoxicity of diospyrin derivatives against EAC tumor cells<sup>6</sup>

Compound	R	R <sup>1</sup>	R <sup>2</sup>	R <sup>3</sup>	IC <sub>50</sub> (μM) (±SE)	GOLD Fitness Score
1 (diospyrin)	H	H	H	H	0.84 ± 0.01	29.84
2	CH <sub>3</sub>	H	CH <sub>3</sub>	H	0.71 ± 0.02	33.69
3	CH <sub>3</sub>	H	CH <sub>3</sub>	NH- <i>p</i> -C <sub>6</sub> H <sub>4</sub> Cl	0.25 ± 0.01	37.09
4	CH <sub>3</sub>	NH <sub>2</sub>	CH <sub>3</sub>	NH <sub>2</sub>	0.24 ± 0.04	31.78
5	CH <sub>3</sub>	H	CH <sub>3</sub>	NH <sub>2</sub>	0.35 ± 0.03	34.24
6	CH <sub>3</sub>	H	CH <sub>3</sub>	NHCOCH <sub>3</sub>	0.06 ± 0.02	38.51
7	CH <sub>3</sub>	H	CH <sub>3</sub>	NHCH <sub>2</sub> C <sub>6</sub> H <sub>5</sub>	1.41 ± 0.07	25.37
8	CH <sub>3</sub>	H	CH <sub>3</sub>	NHCH <sub>2</sub> CH <sub>2</sub> OH	1.07 ± 0.09	33.47
9	CH <sub>3</sub>	H	CH <sub>3</sub>	NHCH <sub>2</sub> CO <sub>2</sub> Et	0.09 ± 0.01	37.50
10	CH <sub>3</sub>	H	CH <sub>3</sub>	NH-β-Naphthyl	0.24 ± 0.04	37.95
11	CH <sub>3</sub>	H	CH <sub>3</sub>	NHCOC <sub>6</sub> H <sub>5</sub>	0.28 ± 0.02	36.47
12	CH <sub>3</sub>	H	CH <sub>3</sub>	NHCOC(CH <sub>3</sub> ) <sub>3</sub>	0.07 ± 0.01	39.39

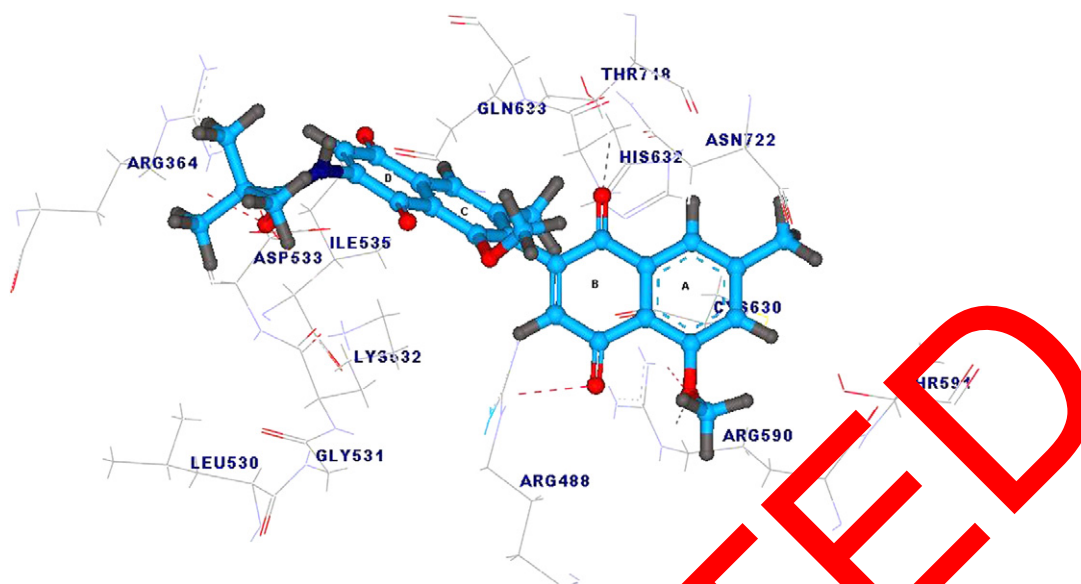


**Figure 2.** Binding interaction of compound 12 with human TopoI, docked using GOLD 3.01. Intermolecular hydrogen bonds and van der Waals interactions are shown as red and gray dashed lines, respectively.

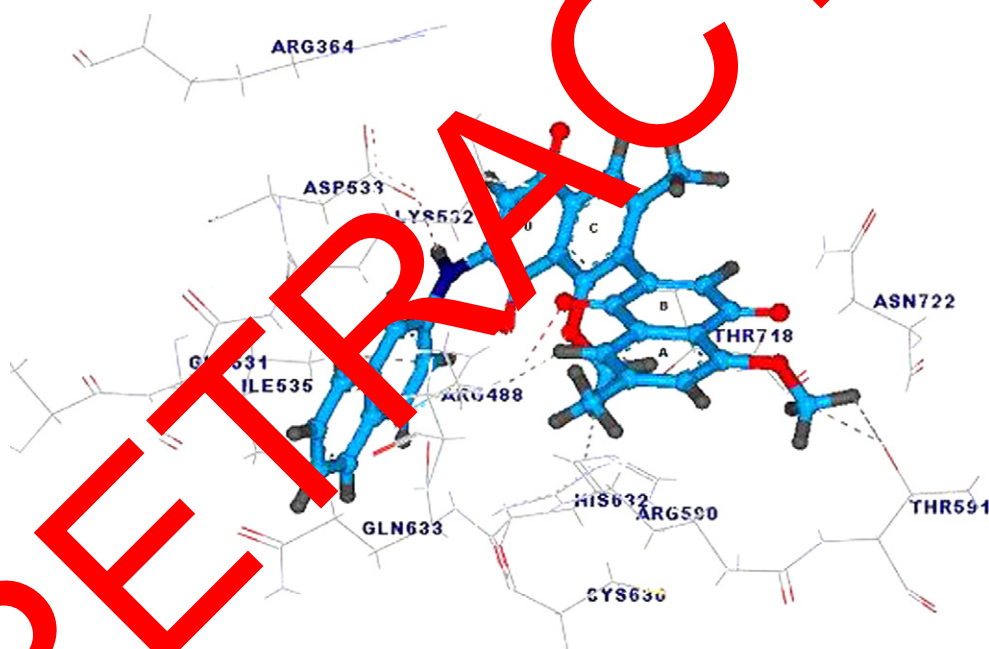


**Figure 3.** Binding interaction of compound 10 with human TopoI, docked using GOLD 3.01. Intermolecular hydrogen bonds and van der Waals interactions are shown as red and gray dashed lines, respectively.

3, respectively, as examples. The carbonyl oxygen at the position 4 of ring B acts as a hydrogen-bond acceptor and forms H-bond with Arg488 (in compounds 1, 2, 4, 6–8, and 10, 12 as shown in Figs. 2 and 3), Arg590 (in compounds 3 and 9), and Thr718 (in compounds 5 and 11).

Residues Asn722, Cys630, His632, and Thr591 were found to surround ring A/B within the van der Waals radius (2.5 Å) and make hydrophobic contacts with these molecules in different docked conformations. Whereas, the carbonyl oxygen and amine linkers in ring C and

D were found within H-bonding distance of residues Arg364, Gln633, and Asp533, in different inhibitors of this series. Interestingly, only the most active compounds 6, 9 and 12 ( $IC_{50} < 0.1 \mu M$ ) were found to interact with Arg364 via H-bonding between amide group (compounds 6 and 12) or ester group carbonyl oxygen (compound 9) and –NH group of Arg364 (Fig. 2 showing binding of compound 12). However this interaction was absent in compound 11 in spite of the presence of an amide group, possibly due to the unfavorable aromatic group at the R<sup>3</sup> substitution. Such an interaction explains the need of a bulky linear substituent with



appropriate electron withdrawing substituent at this position which is evident with the trend shown by the activities of molecules  $11 < 9 < 12 < 6$ . Additionally, the naphthoquinone moiety (ring C/D) of each compound participates in non-polar (van der Waals) interactions with the residues Lys 532, Ile 535, and Gln531. The moderate and less active compounds (**1–5**, **7**, **8**, **10**, and **11**) have  $IC_{50}$  between 0.24 and 1.41  $\mu$ M (Table 1). Their docked structures occupy approximately the same space in the ligand-binding pocket as the more potent compounds, but their naphthoquinone moieties (ring C/D) do not all lie in a single plane and they also lack the favorable interaction with Arg364, which was seen only with the more potent compounds.

As mentioned above, all these compounds are analogues of compound **1** (diospyrin). Introduction of various substituents at position 3' of ring D in these compounds modulates the cytotoxicity of compounds **3–12** as reported in our previous study.<sup>6</sup> To observe the location of predicted binding models within the DNA/TopoI complex, coordinates of DNA were superimposed on each of the ligand–TopoI complex. We found that the naphthoquinone moiety (ring A/B) of compounds (**3–12**) pointed in the direction of Asn722, while the other naphthoquinone moiety (ring C/D) having bulky substitution at 3' position pointed toward the backbone of

DNA non-scissile strand (shown in Fig. 4A). In contrast, these two naphthoquinone rings have entirely different orientation in the parent compound diospyrin, that is, the C/D ring points in the direction of Asn722, while the ring A/B of the molecule lies away from the backbone of DNA non-scissile strand (shown in Fig. 4B). This observation may explain why most of the 3' substituted analogues are more potent than diospyrin. Moreover, the dihedral angle between A/B and C/D rings was found to be in the range of 110–120° for more potent compounds. It seems that this dihedral angle enables ring C/D (which have bulky substitution) to get such conformation that is oriented toward the DNA non-scissile strand.

Figure 5 shows a plot of the calculated GOLD Fitness Scores (binding affinity) for compounds **1–12** against  $IC_{50}$  (Table 1). GOLD Fitness Score consists of protein–ligand hydrogen bond energy, protein–ligand van der Waals energy, ligand–internal hydrogen bond (vdw) energy, and ligand torsional energy terms. It uses Lennard-Jones functional forms for both the external and internal van der Waals contributions to the fitness function.<sup>12</sup> The docking scores for compounds **1–12** correlate reasonably well with the ligands experimental cytotoxicity values giving a correlation coefficient of 0.778. This corroborates with the experimental results

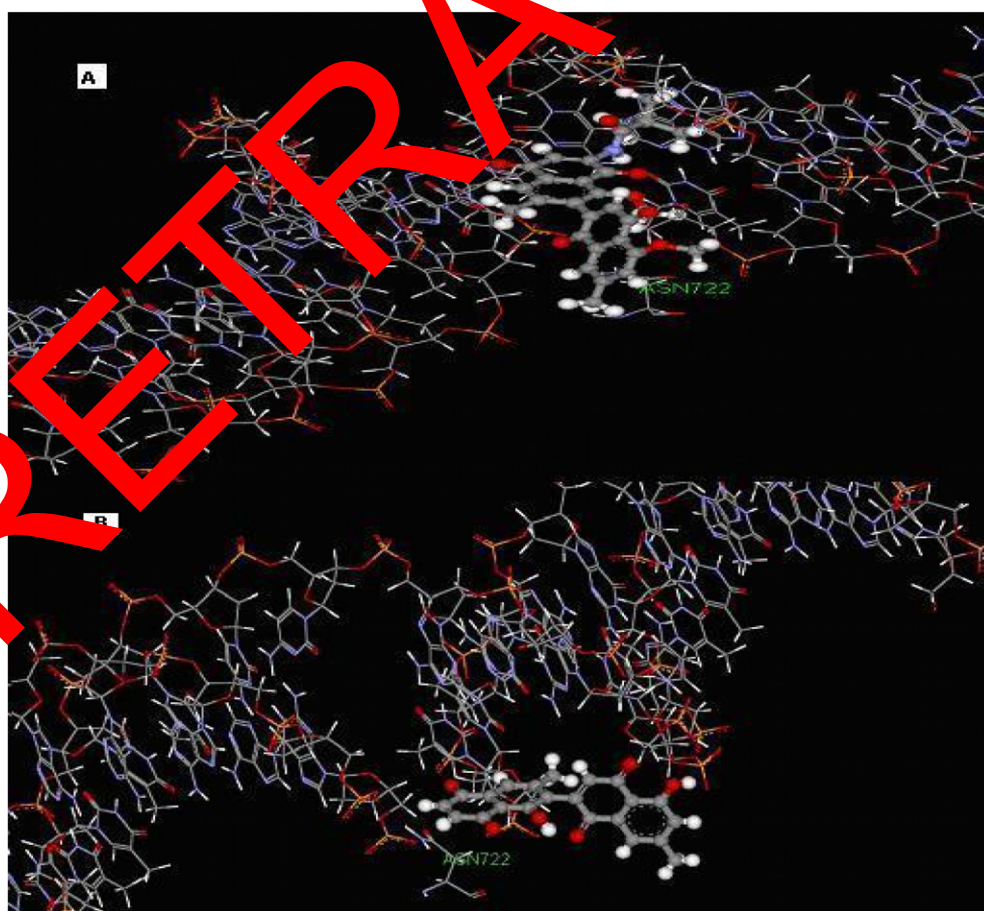


**Figure 4.** Docked orientations of compound **12** (A) and diospyrin (B) within human DNA–TopoI. Only DNA (line), amino acid residue Asn722 (line), and inhibitors (ball and stick) are shown for clarity.

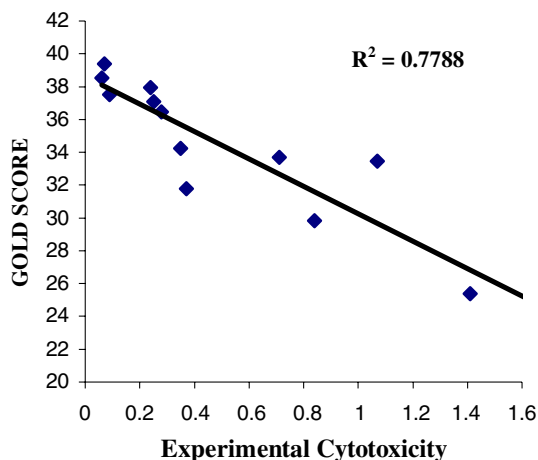


**Figure 5.** Correlation between the calculated GOLD Fitness Score and the experimental activities ( $IC_{50}$ ) of diospyrin derivatives.

obtained in a previous study on African trypanosomes, where cytotoxicity was correlated with the increasing level of cleavable complexes in trypanosomes, implicating topoisomerase-I as the sole intracellular target for these compounds.<sup>22</sup> The reasonable correlation for these ligands further suggests that our predicted binding models may be useful for the understanding of ligand binding to the topoisomerase enzyme and for the design of optimized inhibitors.

Additionally, our docking studies led to the identification of a set of residues in the human-TopoI receptor involved in ligand binding. Several residues were implicated in binding for majority of the ligands including Arg 488, Arg 590, Asp 533, Arg 364, and Lys 532. The involvement of these residues has also been suggested through extensive experimental studies at the topoisomerase receptor and structure-activity relationships studies of other topoisomerase inhibitors.<sup>17,19,20</sup> The purpose of the present study is to propose the binding mode using a more quantitative explanation to the structure-activity relationship of these inhibitors.

**Docking with leishmanial topoisomerase I.** The structural difference between the human and leishmanial type-I DNA topoisomerase (*LdTopoI*) make this enzyme an attractive target for chemotherapeutic intervention.<sup>24</sup> Diospyrin inhibition is relatively specific for *LdTopoI*. On the contrary it requires a 10-fold higher concentration to inhibit the mammalian DNA topoisomerase-I and fails to inhibit *L. donovani* DNA topoisomerase II. Earlier experimental studies suggest that diospyrin, in presence of camptothecin, stimulates the formation of covalent enzyme–DNA complexes in *L. donovani* and induces stabilization of the ‘cleavable complex’ mediated by topoisomerase-I.<sup>21</sup> These observations suggest an important clinical application of this compound,<sup>3,7</sup> making the present study highly relevant.

A comparison of these two enzyme structures revealed that human TopoI is a monomeric enzyme composed of a single 765 residue polypeptide chain, whereas *LdTo-*

poI (PDB:2B9S) is expressed from two open-reading frames to produce a heterodimer consisting of a larger 635 residue subunit and a smaller 262 residue subunit. The large subunit of *LdTopoI* contains a short non-conserved N-terminal domain (start-Met-Glu-43) followed by the conserved core domain (Arg-44–Lys-456) ending in a long C-terminal extension (Val-457–Val-635). The core region of the leishmanial enzyme conserves all the amino acids that characterize the active site of TopoI topoisomerases, such as Arg-314, Lys-352, Arg-410, and His-453. On the other hand, the small *LdTopoI* subunit contains a large non-conserved N-terminal extension (start-Met-Asn-210) enriched in serine residues, which could be phosphorylated. The C-terminal domain starts at Lys-211 and contains the Met-222 required for DNA cleavage.<sup>7,9</sup> The proposed catalytic residues of *LdTopoI* include Arg-314, Arg-410, Lys-352, His-453, and Tyr 222.<sup>7,9</sup> As the antileishmanial activities were not available for all the compounds used in this study, only the parent molecule (1) was used to study the binding mode in *LdTopoI*.

As depicted in Figure 6B, diospyrin was found to make the following interactions with active site residues: (i) hydroxyl group of A-ring of naphthoquinone moiety acts as hydrogen bond acceptor and interacts with backbone –NH of Val315 of the core region (NH–O distance 2.95 Å). (ii) Ring B lies in van der Waals radius of Arg-410 and makes hydrophobic contacts with the core region. (iii) Hydroxyl group of ring-C makes hydrogen bond with Arg-314 (H-bond distance 2.96 Å). (iv) D-ring carbonyl oxygen at 4' position was also found within H-bonding distance of the residues Arg-314 (H-bond distance 2.72 Å) and Lys 352 (H-bond distance 2.52 Å) which are considered essential for inhibitory activity. (v) Naphthoquinone moiety (Ring C/D) stacked between the core region and C-terminal domain, establishing a  $\pi$ – $\pi$  stacking interaction between the aromatic residue Tyr 222 and C-Ring of naphthoquinone moiety. Moreover, one more intermolecular hydrophobic contact between the D-ring carbonyl oxygen at 1' position and Asn 221 seems to stabilize this configuration. The interactions with Tyr 222 and Asn 221 seem to be very important, as these residues stimulate the formation of the covalent enzyme–DNA complexes in *L. donovani* and induce the stabilization of this complex.

The observed selectivity<sup>3</sup> of diospyrin for the leishmanial TopoI over human TopoI can be explained by the differential interactions of this inhibitor with catalytic domains of these two enzymes. The binding interactions are shown in Figure 6A and B. It is suggested through experimental studies that in the core domain of human TopoI, an amino acid ‘tetrad’ consisting of Arg-488, Lys-532, Arg-590, and His-632 constitutes the active site of the enzyme for catalytic activity.<sup>7</sup> This region is essential for the relaxation of supercoiled DNA and shows a high degree of phylogenetic conservation, particularly with respect to residues that interact closely with the double helix. In our docking study diospyrin was found to interact through H-bonding only with Arg 488 of this ‘tetrad’, along with other residues of active site (Fig. 6A). However the derivatives of diospyrin under

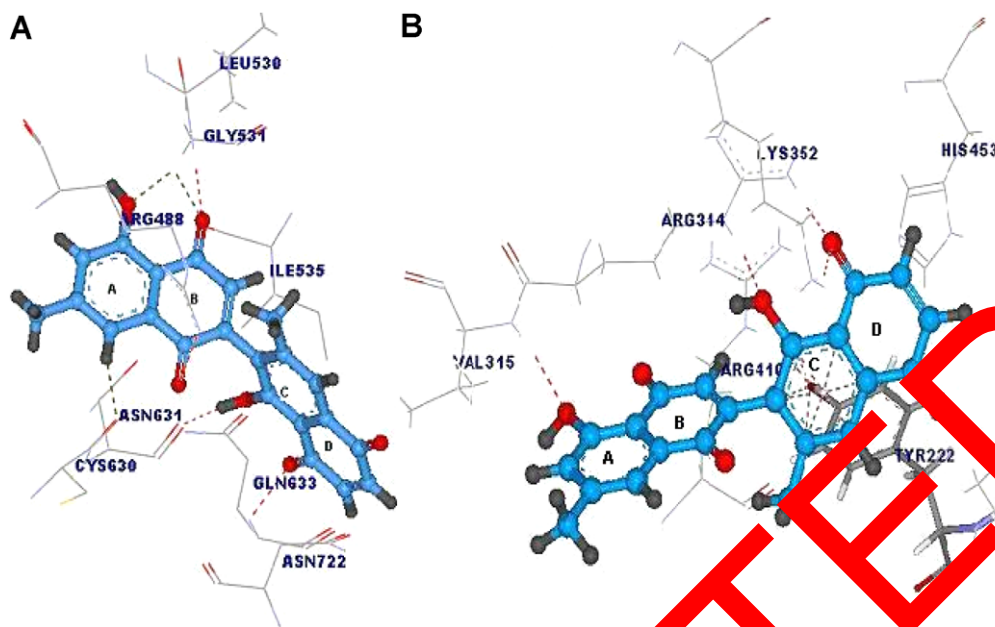


**Figure 6.** Binding of diospyrin within human (A) and leishmania *donovani* (B) topoisomerase-I active site. Hydrogen bond and van der Waals interactions are shown as red and gray dashed lines, respectively.

study interact with other amino acid residues of this ‘tetrad’ as described before.

Calculated protein–ligand-binding free energy of this complex (consisting of best-predicted diospyrin ‘binding model’ in human TopoI) was found to be  $-65.40$  kcal/mol in the form of potential of mean force (PMF) scoring function. PMF score is defined as the sum of the distance-dependent Helmholtz free interaction energies over all interatomic pairs of the protein–ligand complex.<sup>25,26</sup> A higher PMF value indicates a higher protein–ligand-binding affinity. GOLD Fitness Score of this pose was 29.84 as mentioned in Table 1.

Relatively, the core region of the leishmanial enzyme shows a conservation of all the amino acids that characterize the active site of TopoI topoisomerases, such as Arg-314, Lys-352, Arg-410, and His-453 which are homologous to the catalytic ‘tetrad’ of the human enzyme as mentioned before. The molecular docking study of diospyrin with *LdTopoI* clearly identify (Fig. 6B) the residues involved in the binding site interaction and are very similar to those suggested through experimental data. The only observed difference is that instead of His-453, this model shows a  $\pi$ – $\pi$  stacking interaction with aromatic residue of Tyr-222. There is an additional close contact between Asn 221 and the carbonyl group of the naphthoquinone moiety (Ring D). The PMF score for this pose was found to be  $-75.05$  kcal/mol, whereas the GOLD Fitness Score was 50.45. We found that both the above docking scores for *LdTopoI*–diospyrin complex were higher than those for the human TopoI–diospyrin complex and validate the higher selectivity of this inhibitor for *LdTopoI*. The difference in inhibitory effects of diospyrin observed at the structural level of TopoI could be exploited for the development for parasite-specific derivatives.

Based on the above mode of interaction, we generated a structure-based pharmacophore model (Fig. 7) using diospyrin–*LdTopoI* complex. Structure-based pharmacophore generation uses the spatial information of the target protein for topological description of ligand–receptor interactions, which in turn may be used for subsequent discovery of new structural leads by virtual screening or structure-based drug design. The results obtained suggest that the important features in the pharmacophore are: two aromatic centers, three hydrophobic pharmacophore sites, three hydrogen bond acceptors along with excluded volumes of ligand–receptor interaction site of *LdTopoI*. Excluded volume spheres (forbidden sites) provide further restriction and enhanced steric selectivity to a pharmacophore model as the ligand is not allowed to penetrate into these sites of the model.

Chemical features were centered onto the amino acids Arg 314, Lys 352 and Val 315 surrounding the carbonyl and hydroxyl groups of the ligand, and onto Arg 410, Tyr 222, Asn 221 which form the hydrophobic pocket around the naphthoquinone moiety (ring C/D). This observation suggests that these binding points are mapped onto the model of the topoisomerase-binding site, as shown in Figure 7, which is in good agreement with the binding mode of diospyrin (Fig. 6B). It should be noted that diospyrin uses almost all of the pharmacophore sites in interacting with the *LdTopoI* receptor. This structure-based pharmacophore built from the protein active site can be used as query to search new compounds that share a set of common features responsible for the inhibition of *LdTopoI*.

In conclusion, our studies give structural insights about the plausible binding modes for diospyrin and its amino derivatives with the human TopoI and diospyrin itself



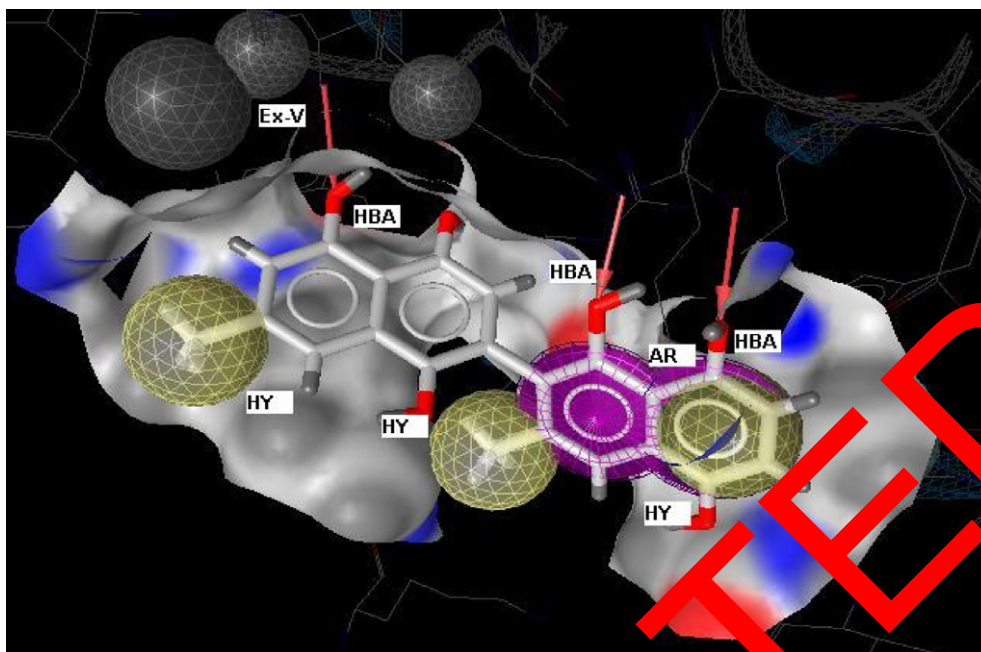


**Figure 7.** Structure-based pharmacophore hypothesis based on diospyrin–*LdTopoI* complex, derived using LigandScout v3.01 program. Active site shown as surface around pharmacophore, consisting of two aromatic points (purple), three hydrophobic points (yellow), and three vectorized hydrogen bond acceptors (red); with excluded volume spheres (gray).

with the leishmanial TopoI. Selection of ‘best’ binding models was made based on the scoring functions and agreement between different docking methods. The results led to a proposed pharmacophore model, for antileishmanial activity, consisting of two aromatic regions, three hydrophobic areas, three hydrogen bond acceptor sites along with excluded volumes within the *LdTopoI* residues in the binding site. The results suggest that in absence of complete information on the diospyrin/DNA topoisomerase binding interactions, alternative computational strategies viz., virtual screening and SBDD may be productively used for identifying new and selective leishmanial-topoisomerase inhibitors. The result obtained in this study contributes to the understanding of the mode of action of TopoI inhibition by diospyrin and its amino derivatives in the human host cells and that of diospyrin in the parasite *L. donovani*. The differential interactions of these inhibitors with *L. donovani* and human TopoI indicate the existence of sufficient biochemical and structural differences to enable selective targeting of the parasite enzyme. Work in this direction is under progress.

#### Acknowledgment

Authors are thankful to Council for Scientific and Industrial Research (CSIR), New Delhi, India, for financial assistance.

#### References and notes

- Jean-Moreno, V.; Rojas, R.; Goyeneche, D.; Coombs, G. H.; Walker, J. *Exp. Parasitol.* **2006**, *112*, 21.
- Lauria, A.; Ippolito, M.; Almerico, A. M. *J. Mol. Model.* **2006**, *13*, 393.
- Das, S. M.; Hazra, B.; Mittra, B.; Das, A.; Majumdar, H. K. *Mol. Biochem. Pharmacol.* **1998**, *54*, 994.
- Ganapaty, S.; Steve, T. P.; Karagianis, G.; Waterman, P. Brun, R. *Phytochemistry* **2006**, *67*, 1950.
- Banly, C. *Curr. Med. Chem.* **2000**, *7*, 39.
- Das, S. M.; Ghosh, R.; Patra, A.; Sharma, P.; Ghoshal, N.; Hazra, B. *Bioorg. Med. Chem.* **2006**, *12*, [Epub ahead of print].
- Reguera, R. M.; Redondo, C. M.; Gutierrez de Prado, R.; Pérez-Pertejo, Y.; Balaña-Fouce, R. *Biochimica. Biophysica. Acta* **2006**, *1759*, 117.
- Staker, B. L.; Feese, M. D.; Cushman, M.; Pommier, Y.; Zembower, D.; Stewart, L.; Burgin, A. B. *J. Med. Chem.* **2005**, *48*, 2336.
- Davies, D. R.; Mushtaq, A.; Interthal, H.; Champoux, J. J.; Hol, W. G. *J. Mol. Biol.* **2006**, *357*, 1202.
- MSI Cerius2 Version 4.9, Molecular simulations, Accelrys Inc., 9685 Scranton Rd., San Diego, CA 92121, USA.
- Rappe, A. K.; Casewit, C. J.; Colwell, K. S.; Goddard, W. A.; Skiff, W. M., III *J. Am. Chem. Soc.* **1992**, *114*, 10024.
- GOLD 3.0; Cambridge Crystallographic Data Centre: Cambridge, CB2 1EZ, UK.
- Jones, G.; Willett, P.; Glen, R. C.; Leach, A. R.; Taylor, R. *J. Mol. Biol.* **1997**, *267*, 727.
- Verdonk, M. L.; Cole, J. C.; Hartshorn, M. J.; Murray, C. W.; Taylor, R. D. *Proteins Struct. Funct. Genet.* **2003**, *52*, 609.
- Maple, J. R.; Hwang, M. J.; Stockfish, T. P.; Dinur, U.; Waldman, M.; Ewig, C. S.; Hagler, A. T. *J. Comput. Chem.* **1994**, *15*, 161.
- (a) Mehler, E. L.; Solmajer, T. *Protein Eng.* **1991**, *4*, 903; (b) Leach, A. R. In *Molecular Modelling: Principles and Applications*; Pearson Edu. Ltd: England, 2001; pp 165–252, Chapter 4.
- Sharma, P.; Ghoshal, N. *J. Chem. Inf. Model* **2006**, *46*, 1763.
- Wolber, G.; Langer, T. *J. Chem. Inf. Model.* **2005**, *45*, 160.
- Stewart, L.; Ireton, G. C.; Champoux, J. J. *J. Biol. Chem.* **1996**, *271*, 7602.



20. Stewart, L.; Ireton, G. C.; Champoux, J. J. *J. Mol. Biol.* **1997**, 269, 355.
21. Tazi, J.; Bakkour, N.; Soret, J.; Zekri, L.; Hazra, B.; Laine, W.; Baldeyrou, B.; Lansiaux, A.; Bailly, C. *Mol. Pharmacol.* **2005**, 67, 1186.
22. Bodley, A. L.; Wani, M. C.; Wall, M. E.; Shapiro, T. A. *Biochem. Pharmacol.* **1995**, 50, 937.
23. Chessman, S. J. *Parasitol. Today* **2000**, 16, 277.
24. Bakshi, R. P.; Shapiro, T. A. *Mini-Rev. Med. Chem.* **2003**, 3, 597.
25. Muegge, I.; Martin, Y. C.; Hajduk, P. J.; Fesik, S. W. *J. Med. Chem.* **1999**, 42, 2498.
26. Irene, N.; Mitchell, J. B. O.; Alexander, A.; Thornton, J. *J. Comput. Chem.* **2001**, 22, 673.

RETRACTED